

Reflection of plane elastic waves in tetragonal crystals with strong anisotropy

Vitaly B. Voloshinov^{a)} and Nataliya V. Polikarpova^{b)}

Department of Physics, M. V. Lomonosov Moscow State University, 119991 Moscow, Russia

Nico F. Declercq^{c)}

George W. Woodruff School of Mechanical Engineering, Georgia Institute of Technology, 801 Ferst Drive, Atlanta, Georgia 30332-0405 and Laboratory for Ultrasonic Nondestructive Evaluation Office 304, UMI Georgia Tech-CNRS 2958, Georgia Tech Lorraine, 2 rue Marconi, 57070 Metz-Technopole, France

(Received 24 April 2008; revised 20 November 2008; accepted 22 November 2008)

Propagation and reflection of plane elastic waves in the acousto-optic crystals tellurium dioxide, rutile, barium titanate, and mercury halides are examined in the paper. The reflection from a free and flat boundary separating the crystals and the vacuum is investigated in the (001) planes in the case of glancing acoustic incidence on the boundary. The analysis shows that two bulk elastic waves may be reflected from the crystal surface. The energy flow of one of the reflected waves in paratellurite and in the mercury compounds propagates in a quasi-back-direction with respect to the incident energy flow. It is proved that energy flows of the incident and reflected elastic waves are separated by a narrow angle of only a few degrees. It is also found that the relative intensity of the unusually reflected waves is close to a unit in a wide variety of crystal cuts. General conclusions related to acoustic propagation and reflection in crystals have been made based on the examined phenomena in the materials. © 2009 Acoustical Society of America. [DOI: 10.1121/1.3050307]

PACS number(s): 43.35.Sx, 43.20.Ef [OAS]

Pages: 772–779

I. INTRODUCTION

Even though it is known that there exists a strong acoustic energy walk-off in certain crystalline materials, the influence of the walk-off on the process of reflection in terms of direction and intensity has not been profoundly studied before. This paper examines regular trends of propagation and unusual reflection of harmonic homogeneous plane elastic waves in a family of tetragonal dielectric crystals. The crystalline materials chosen for the analysis are widely used in modern acousto-optic devices intended for applications in optical engineering and laser technology.^{1–3,17} In particular, the crystals considered in this paper are tellurium dioxide (TeO₂), mercury halides (Hg₂Cl₂, Hg₂Br₂, and Hg₂I₂), rutile (TiO₂), and barium titanate (BaTiO₃). It was found that the crystals based on mercury and tellurium demonstrate extremely strong anisotropy of their elastic properties. On the contrary, rutile and barium titanate, similar to the majority of acoustic crystalline materials, are characterized by a moderate and low grade of anisotropy.^{1–7}

It is known that the phase velocity of bulk acoustic waves V strongly depends on the direction of propagation in crystals possessing pronounced elastic anisotropy.^{4–9} For example, a slow-shear acoustic wave propagating in the XY plane of tellurium dioxide at the angle $\theta=45^\circ$ relative to the axis X has an extraordinary low magnitude of the phase velocity $V=616$ m/s. However, the same acoustic mode sent along the axis X of the material is characterized by a velocity

up to five times higher $V=3050$ m/s.^{1–3} As for the crystals with a low grade of anisotropy, the ratio r of maximal and minimal velocity magnitudes does not exceed a factor of 2 yielding the square of this ratio $A=4.0$.^{1,2}

Elastic waves propagating in strongly anisotropic crystals are characterized by large walk-off angles ψ between the vectors of phase V and group V_g velocities of ultrasound.^{1–10} It was found that the walk-off angle ψ between the acoustic wave vector K and the energy flow (Poynting) vector in these materials might reach magnitudes $\psi>70^\circ$. On the other hand, in crystals with moderate and low anisotropy, e.g., in BaTiO₃, the walk-off angle is limited to $\psi=50^\circ$.^{1–16} As recently predicted theoretically^{13,14} and confirmed experimentally in the crystals of tellurium dioxide,¹⁵ propagation of waves with large acoustic walk-off angles may give rise to a significant unusual reflection of the elastic energy from a free boundary separating the material and the vacuum.^{15,16}

In this paper, the peculiar reflection of bulk and plane elastic waves is studied in the XY plane of the acousto-optic materials though the analysis may easily be extended to crystals of other classes. In order to examine regular trends of unusual reflection and to reveal the influence of elastic anisotropy on the reflection process, the investigation was carried out not in a single but in a family of crystalline materials characterized by a different grade of elastic anisotropy.

II. GLANCING INCIDENCE AND REFLECTION IN CRYSTALS

The analysis carried out in this paper is related to a rather peculiar case of acoustic reflection in crystals when a crystalline specimen is cut in the form of a rectangular prism. Figure 1 shows the rectangular specimen of a tetragonal

^{a)}Electronic mail: volosh@phys.msu.ru

^{b)}Electronic mail: polikarp@phys.msu.ru

^{c)}Author to whom correspondence should be addressed. Electronic mail: nico.declercq@me.gatech.edu

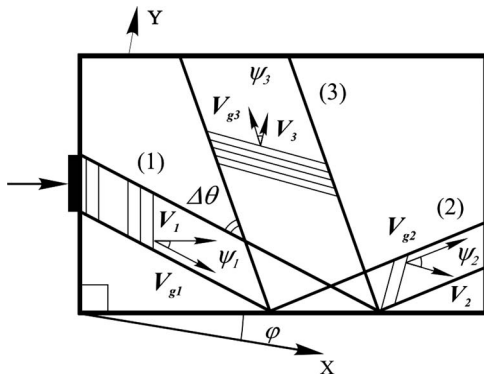


FIG. 1. General scheme of reflection in crystals with strong anisotropy.

crystal and the piezoelectric transducer bonded to the left side facet of the crystal. It is considered that the transducer generates a quasilongitudinal or quasishear acoustic wave (1) in the crystal. It is also assumed that the incident wave possesses a phase velocity vector V_1 and a corresponding wave vector K_1 directed at the angle φ relative to the X-axis [100]. As illustrated, the acoustic beam (1) propagates in the material at a walk-off angle ψ_1 evaluated between the vectors of phase velocity V_1 and group velocity V_{g1} of ultrasound. After propagation through the crystal, the acoustic energy is incident on the bottom facet of the specimen. This facet of the crystal serves as a solid-vacuum interface. Therefore the acoustic energy of the (bulk) harmonic homogeneous plane elastic wave is incident on a free and smooth, homogeneous surface.

According to everyday experience, one would be tempted to intuitively predict that the reflected beam (2) propagates from the bottom surface of the crystal away from the direction of the acoustic incidence. However, as seen in the figure, the beam (2) is characterized by the walk-off angle ψ_2 . This angle is evaluated between the wave vector K_2 , or the phase velocity vector V_2 , on the one hand, and the group velocity vector V_{g2} , on the other hand. However, it was recently found¹³⁻¹⁶ that, in addition to the traditionally reflected beam (2), there appears an unusually reflected beam (3). It possesses a phase velocity vector V_3 corresponding to the wave vector K_3 . The extraordinary reflected beam (3) and

the incident ray (1) are separated in space by the space separation angle $\Delta\theta$. As predicted in Refs. 6, 13, and 14, one of the two reflected waves, in particular, the wave (3), may propagate approximately toward the incident acoustic ray, i.e., in back direction relative to the direction of the incidence.

III. PHASE VELOCITIES OF ULTRASOUND IN THE XY-PLANE OF CRYSTALS

In order to understand the origin of the unusual reflection in the crystals, the dependences of magnitudes $V(\theta)$ of the acoustic phase velocities on the direction of propagation in the XY-plane of tetragonal materials were calculated. The velocity vectors of the quasishear acoustic waves V_s and the quasilongitudinal acoustic waves V_l propagating at the angle θ relative to the axis [100] have been obtained from Christoffel's equation.^{1,2} The elastic coefficients of the materials used in the calculations are summarized in Table I. Data on the coefficients were found in the literature.^{1-3,5}

It is shown^{1,2,11-14} that the value of the acoustic phase velocity of waves in the XY-plane of the crystals can be expressed as

$$V_{1,2}^2 = (1/2\rho)(c_{11} + c_{66} \pm \sqrt{(c_{11} - c_{66})^2 \cos^2 2\theta + (c_{12} + c_{66})^2 \sin^2 2\theta}), \quad (1)$$

$$V_3^2 = c_{44}/\rho.$$

The acoustic slowness curves¹ $1/V_1$ and $1/V_2$ in the XY-plane of BaTiO₃ and TiO₂ are plotted in Figs. 2(a) and 2(b) while data in Figs. 2(c) and 2(d) illustrate the acoustic slowness curves corresponding to Hg₂Cl₂ and TeO₂. It can also be seen that paratellurite and calomel definitely demonstrate a very strong anisotropy of their elastic properties compared to TiO₂ and BaTiO₃. The ratios A of the second power of the maximum and minimum magnitudes describing the shear velocities V_2 in the XY-plane of calomel and tellurium dioxide are equal to $A=22.1$ and $A=24.0$. In comparison, the single crystal of barium titanate possesses a velocity ratio $A=2.3$. As for the crystals of TiO₂, they are characterized by the coefficient $A=4.0$. It is quite evident that the

TABLE I. Density and elastic coefficients of tetragonal crystals.

Crystal	Density (10 ³ kg/m ³) ρ	Elastic coefficients (10 ¹⁰ N/m ²)					
		c_{11}	c_{12}	c_{13}	c_{33}	c_{44}	c_{66}
Barium titanate (BaTiO ₃)	6.00	27.5	17.9	15.2	16.5	5.43	11.3
Rutile (TiO ₂)	4.30	27.3	17.6	14.9	48.4	12.5	19.4
Paratellurite (TeO ₂)	6.00	5.60	5.15	2.20	10.6	2.65	6.60
Calomel (Hg ₂ Cl ₂)	7.18	1.89	1.71	1.56	8.03	0.84	1.22
Mercury bromide (Hg ₂ Br ₂)	7.31	1.61	1.50	1.88	8.88	0.74	1.11
Mercury iodide (Hg ₂ I ₂)	7.70	1.42	1.32	2.20	10.70	0.58	1.11

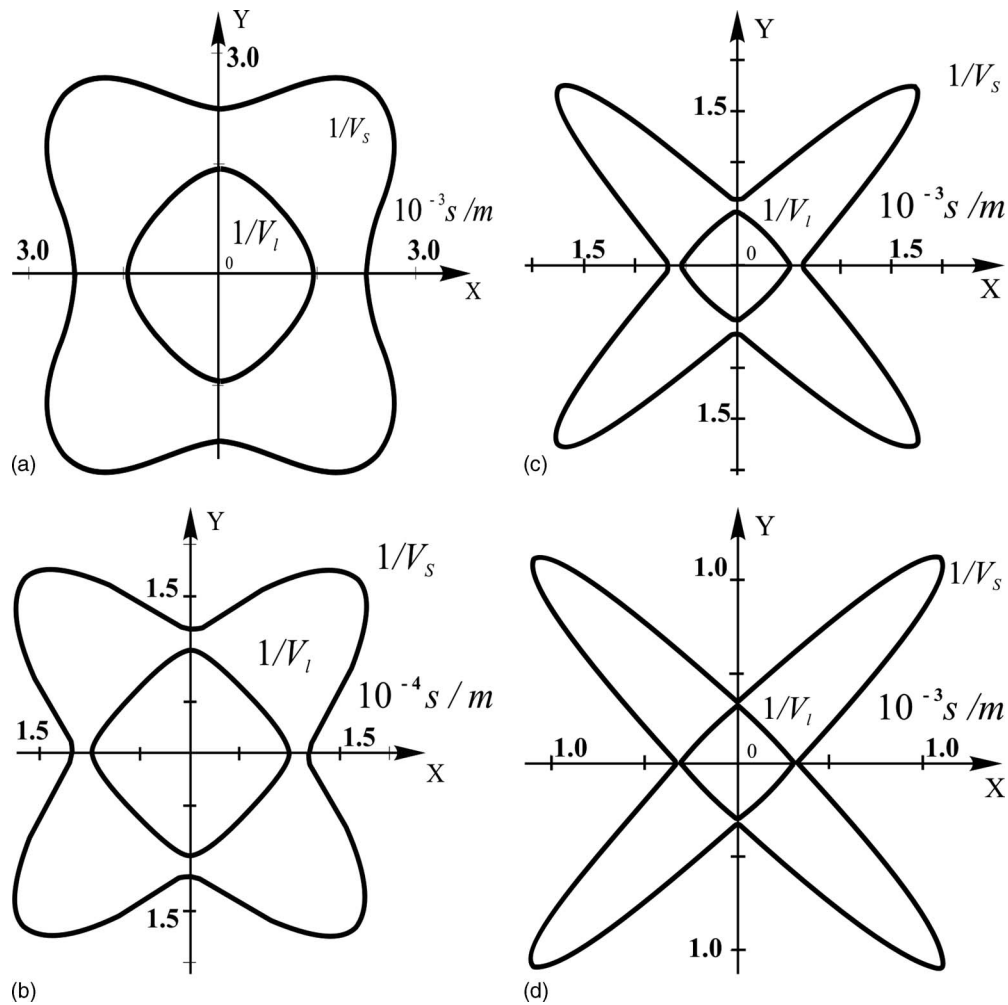


FIG. 2. Acoustic slowness curves in the XY plane of (a) BaTiO_3 , (b) TiO_2 , (c) Hg_2Cl_2 , and (d) TeO_2 .

elastic anisotropy of a crystal may be qualitatively evaluated just from a general view of the acoustic slowness curves.

IV. ACOUSTIC WALK-OFF ANGLE IN THE CRYSTALS

In addition to the magnitudes of the phase velocity V , the acoustic walk-off angles ψ in the XY -plane of the investigated crystals were calculated following the traditional procedure.^{1,2} As proved by the calculations, the maximum acoustic walk-off angle for the slow-shear wave in this plane of tellurium dioxide may be amazingly wide, $\psi=74^\circ$.^{4,8-10} On the other hand, the quasilongitudinal mode with a velocity value V_1 possesses a smaller walk-off angle $\psi=35^\circ$. As for the mercury halides, the behavior of the acoustic waves, in many aspects, is similar to paratellurite. For example, the maximum walk-off angle in the XY -plane of Hg_2Cl_2 is equal to $\psi=70^\circ$. In the other two mercury materials, i.e., mercury bromide and mercury iodide, the magnitudes of the maximum walk-off angles are between the limits $\psi=70^\circ$ and $\psi=74^\circ$. In barium titanate and rutile, the acoustic walk-off angles are less than $\psi=50^\circ$. This regular trend is of importance in understanding the phenomenon of acoustic reflection in crystals.

V. DIRECTIONS OF PROPAGATION OF REFLECTED WAVES

It is seen in Fig. 1 that the energy flow of the acoustic wave (1) generated by the transducer is incident on the bottom facet of the sample. The schematic presented in Fig. 3 shows the directions of the wave vectors \mathbf{K}_2 and \mathbf{K}_3 corresponding to the two reflected beams [(2) and (3)] in Fig. 1. It is indicated in Fig. 1 that the transducer launches the incident

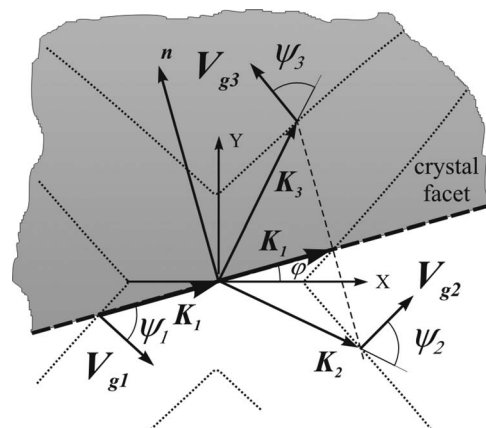


FIG. 3. Directions of wave vectors and group velocities of ultrasound.

wave (1) at the angle φ relative to the axis X . It is also clear that the wave vector \mathbf{K}_1 of the incident beam is directed parallel to the bottom facet of the crystal. This facet is shown in Fig. 3 by the bold dashed line that forms an angle φ with the X -axis. The body of the crystal is shown in Fig. 3 by the gray background, while the boundary is indicated by the label “crystal facet.” The vector \mathbf{n} in the figure is normal to the boundary separating the crystal and the vacuum. The length of the projection of the wave vector \mathbf{K}_1 on the boundary for the incident wave is equal just to the length of the wave vector itself because the specimen is rectangular and the investigated case of acoustic incidence may be defined as glancing or grazing. The projection of this vector on the boundary is shown to the left of the normal.

A. Directions of wave vectors of the reflected beams

According to the general laws of wave theory, directions of the two reflected wave vectors \mathbf{K}_2 and \mathbf{K}_3 in Fig. 3 may be found from the known condition, usually referred to as the law of Snell–Descartes, of equal projections of the incident and reflected wave vectors on the crystal facet.^{1,2,14} Detailed explanations of the method to find the directions of the wave vectors and group velocity vectors are presented in Ref. 14. In order to satisfy the condition of equal projections, a supplementary dashed line is plotted in the figure at the extremity of the vector \mathbf{K}_1 . The vector \mathbf{K}_1 is plotted to the right of the normal \mathbf{n} . This vector is equal to the vector \mathbf{K}_1 shown to the left of the normal. The supplementary line is orthogonal to the boundary and parallel to the normal \mathbf{n} . A dotted line representing the cross section of the acoustic wave vector surface in the XY plane of the crystal may be seen in Fig. 3. This curve directly follows from the slowness curve for the velocity V_S depicted in Fig. 2(d). Data in Fig. 3 prove that the supplementary line intersects with the dotted curve. Moreover, there are as much as two intersections of the supplementary line with the dotted line. As a result, the directions of the two acoustic wave vectors of the reflected waves \mathbf{K}_2 and \mathbf{K}_3 may be found if the intersection points are known. It is common to define the reflected wave (2) corresponding to the wave vector \mathbf{K}_2 as the “ordinary” reflected wave. The wave (3) described by the vector \mathbf{K}_3 may be defined as the “extraordinary” reflected wave. It should be emphasized that the tangential projections, on the boundary, of the wave vectors \mathbf{K}_2 and \mathbf{K}_3 are equal to the length of the wave vector \mathbf{K}_1 plotted to the right of the normal \mathbf{n} . As mentioned, the same vector \mathbf{K}_1 , to the left of the normal, describes the incident wave.

B. Directions of energy flows of the reflected beams

Based on the presented considerations, it is possible to determine in Fig. 3 the directions of the acoustic energy flow before and after the reflection. As seen in Fig. 3, the angle between the acoustic wave vector \mathbf{K}_1 and the Poynting vector of the incident beam (1) is equal to ψ_1 . The picture also shows that the group velocity vector \mathbf{V}_{g1} of the beam (1) is orthogonal to the wave surface in the point where the vector \mathbf{K}_1 touches the surface of the wave vectors to the right of the normal \mathbf{n} . As for the reflected beam (2), the drawing proves

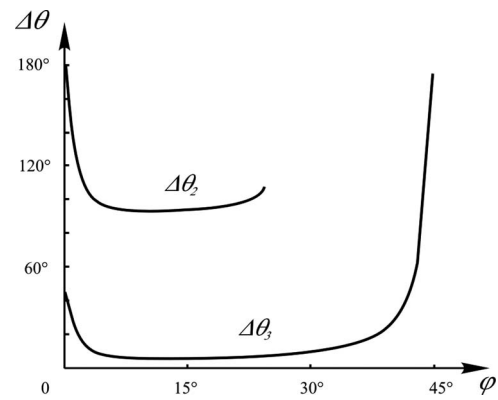


FIG. 4. Separation angle for the slow acoustic mode in TeO_2 .

that the wave vector \mathbf{K}_2 is directed outside the crystal. Therefore, acoustic wave fronts of the wave (2) in Figs. 3 and 1 are tilted clockwise relative to the boundary. On the other hand, the energy flow of the reflected beam (2) propagates at the angle ψ_2 inside the crystal so that the reflected beam is directed away from the boundary and from the incident beam (1).

In order to understand the origin of the peculiar reflection at the boundary, the direction of the group velocity \mathbf{V}_{g3} of the reflected wave (3) must be examined. The unusually reflected wave (3) is represented in Fig. 3 by the wave vector \mathbf{K}_3 and the acoustic walk-off angle ψ_3 . As proved by Fig. 3, the wave vector \mathbf{K}_3 is directed inside the crystal and away from the bottom facet of the specimen. In this respect, the reflection takes place in accordance with the expectations. However, the energy flow of the reflected wave (3) propagates backward with respect to the energy flow of the incident wave (1) because the group velocity vectors \mathbf{V}_{g3} and \mathbf{V}_{g1} are practically directed opposite to each other.

It has been shown recently that the revealed peculiarity originates from the extremely large value of the acoustic walk-off angle ψ_3 while the large walk-off angle is the consequence of the strong elastic anisotropy of the acousto-optic materials under consideration.^{13–16}

VI. THE SPATIAL SEPARATION ANGLE BETWEEN TWO REFLECTED WAVES

The magnitudes of the acoustic walk-off angles ψ_1 , ψ_2 , and ψ_3 in the XY plane of the crystals for the three acoustic waves were calculated. The calculation was carried out for directions of the incident wave propagation corresponding to the cut angle $0 < \varphi < 45^\circ$. In other words, due to the symmetry of the tetragonal crystals, the analysis included practically all orientations of the rectangular sample with respect to the crystalline axes. As for the directions with $\varphi=0$ and $\varphi=45^\circ$, they were not considered because the acoustic waves propagate along these directions without energy walk-off and hence without any reflection from the bottom facet of the specimen.

During the carried out analysis, similar to that presented in this paper,¹⁴ the angles $\Delta\theta_2$ and $\Delta\theta_3$ between the energy flows of the incident (1), the ordinary (2), and the extraordinary (3) reflected slow-shear waves were determined for

TABLE II. Trends of the materials depending on the grade of the elastic anisotropy in tetragonal crystals during the incidence of slow incident acoustic mode.

Crystals	Walk-off angle ψ ($^\circ$)	Anisotropy parameter $A=(V_{\max}/V_{\min})^2$	Separation angle $\Delta\theta_{\min}$ ($^\circ$)	Critical angle φ_c ($^\circ$)	Maximum reflection coefficient R_3
Barium titanate (BaTiO ₃)	$\psi_1=40$	2.3	72.8	9.7	0.05
Rutile (TiO ₂)	$\psi_1=51$	4.0	38.6	14.3	0.43
Mercury bromide (Hg ₂ Br ₂)	$\psi_1=72$	19.4	7.2	23.7	0.96
Calomel (Hg ₂ Cl ₂)	$\psi_1=70$	22.1	9.7	22.324	0.93
Mercury iodide (Hg ₂ I ₂)	$\psi_1=74$	24.0	5.6	24.060	0.97
Paratellurite (TeO ₂)	$\psi_1=74$	24.0	5.3	24.131	1.00

each value of the cut angle φ . The data in Fig. 4 demonstrate the obtained dependences of the separation angles $\Delta\theta_2$ and $\Delta\theta_3$ on the cut angle of the crystals. It may be seen in Fig. 4 that the angle $\Delta\theta_3$ in tellurium dioxide is amazingly small $\Delta\theta_3 \leq 10^\circ$ over the wide range of the cut angles $4^\circ < \varphi < 32^\circ$. It means that there are no strict requirements on the orientation of a specimen in order to observe the peculiar reflection in the crystal. The data in Fig. 4 also represent the behavior of the spatial separation angle $\Delta\theta_2$ for the ordinary reflected wave (2). As proved by the analysis, this wave exists in TeO₂ samples cut at the angle $0 < \varphi < 24^\circ$.

Similar calculations were made for the fast acoustic mode in paratellurite and also in the single crystals of calomel, mercury bromide, and mercury iodide. As found, the separation angle for the extraordinary reflected wave in the crystals also does not exceed the value $\Delta\theta_3 \leq 10^\circ$ in a wide range of cut angles. However, the separation angle between the incident and reflected waves in rutile and barium titanate is equal to dozens of degrees, thus indicating that there is no backreflection of the elastic waves in the crystals with moderate and low anisotropy.

The performed analysis proves that the minimum value of the separation angle in tellurium dioxide occurs as low as $\Delta\theta_3=5.3^\circ$, while in the mercury halides the angle is only slightly wider: in calomel it is limited to $\Delta\theta_3=9.7^\circ$. Therefore, the research revealed that the regular trend of “near backreflection” of acoustic waves is typical for all crystalline materials possessing strong anisotropy of the elastic properties. For example, in the crystal BaTiO₃ the minimum value of the separation angle is as large as $\Delta\theta_3=72.8^\circ$. In the crystal rutile, the angle is equal to $\Delta\theta_3=38.6^\circ$. It means that, in the crystals with moderate anisotropy, the acoustic reflection takes place in the forward and not in the backward direction with respect to the incident energy flow.

The analysis was extended to the cases of glancing incidence and reflection of the fast, i.e., the quasilongitudinal, waves in the tetragonal crystals. Similar to the reflection of the quasishear waves, the separation angles in the materials with the pronounced elastic anisotropy are narrow. It was

also found that one of the two reflected waves in paratellurite is a quasishear acoustic mode while the other wave is a quasilongitudinal mode. The minimal separation angle in TeO₂ is equal to $\Delta\theta_3=5.9^\circ$. In the crystal Hg₂Cl₂, this angle is slightly wider $\Delta\theta_3=12.2^\circ$. However, in the materials with low anisotropy, for example, in BaTiO₃, the separation angle is equal to $\Delta\theta_3=73.9^\circ$. Data on results of calculations of the separation angles for the slow incident acoustic mode are included in Table II. Therefore, based on the carried out analysis, it is possible to conclude that the quasi-back-reflection of the acoustic waves is a phenomenon typical of the quasishear and the quasilongitudinal mode in strongly anisotropic media.

VII. THE DISTRIBUTION OF ELASTIC ENERGY OVER REFLECTED WAVES

Analysis of the phenomenon of the unusual reflection of waves required evaluation of the amount of energy flow reflected from the free and flat boundary in the form of the extraordinary (3) wave. In order to fulfill the analysis, mutual distribution of the incident elastic energy over the two reflected waves was determined. The reflection coefficients R_2 and R_3 describing energy flows of the reflected beams (2) and (3) were calculated for this purpose. The method of calculation of the reflection coefficients was proposed in Ref. 6. Application of the method to the tetragonal crystals is discussed in detail in Refs. 13 and 14. In this paper, we mainly concentrate on discussion of the calculation results related to the chosen family of crystals. Each coefficient was defined as a ratio of the normal projections of the energy flows in the corresponding reflected and incident waves.^{1,2,6} Therefore, it was stated that the following relation $R_2+R_3=1$ was valid in the crystal. It means that the energy of the incident bulk acoustic wave is considered equal to unity. This energy is totally distributed over the energy flows of the two bulk reflected waves. For simplicity, a possibility of appearance of surface and inhomogeneous (evanescent) waves is ignored. The analysis also ignores piezoelectric and other effects that

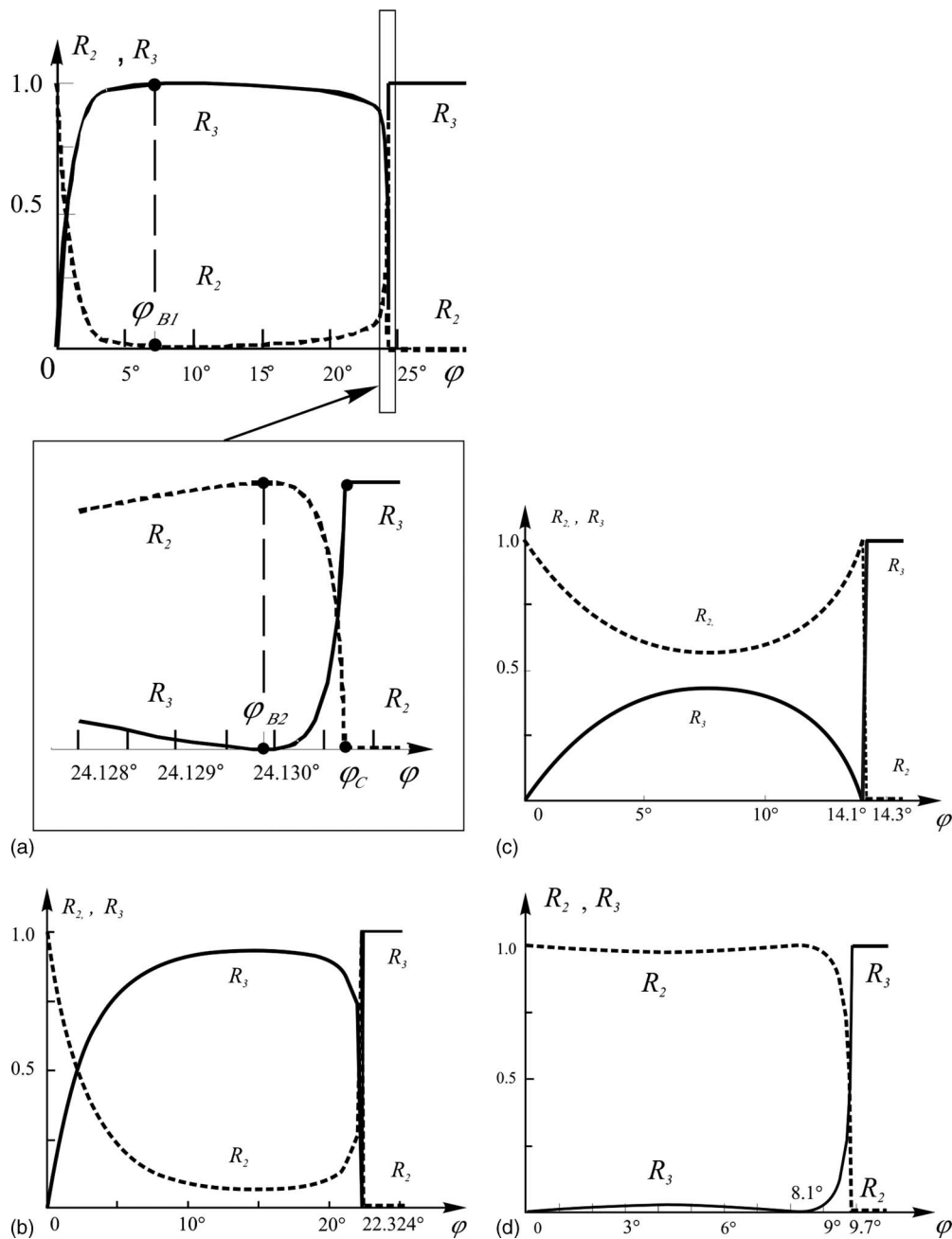


FIG. 5. Reflection coefficients of the slow acoustic mode in the XY plane of (a) TeO_2 , (b) Hg_2Cl_2 , (c) TiO_2 , and (d) BaTiO_3 .

might influence the process of reflection. This is justifiable because in a crystal like tellurium dioxide the piezoelectric effect is relatively small, almost negligible in fact. The complicated calculation required the evaluation of components of the stress tensor and of the acoustic displacement vectors in the examined crystals. For such purposes a relation between the stress tensor represented in the system of coordinates of the boundary and crystalline axes is found.

The data in Fig. 5(a) show calculated dependences of the reflection coefficients R_2 and R_3 on the cut angle φ in tellurium dioxide. It is seen that the range of changes of the cut angles $0 < \varphi < 45^\circ$ for convenience may be divided into four different intervals. These intervals correspond to different types of dependences of the reflection coefficients on the cut angle. The analysis proves that if the crystal is cut at the

angle φ slightly different from zero, the major amount of the incident elastic energy is reflected in the form of the ordinary elastic wave, i.e., the wave (2) in Fig. 1. Growth of the angle φ is accompanied by an increase in the energy flow of the extraordinary reflected wave (3), while the intensity of the forward reflected wave (2) vanishes.

If the propagation angle φ is limited to the range $3 < \varphi \leq 25^\circ$ then the major amount of the reflected energy is concentrated in the extraordinary reflected ray. Calculation proves that at the angle $\varphi_{B1} = 7.5^\circ$ all incident elastic energy is reflected in the quasi-back-direction because the coefficient $R_3 = 1$. Consequently, the cut angle φ_{B1} , similar to optics, may be defined as the Brewster angle. This definition of the angle seems possible because one of the reflected waves, i.e., wave (2), at this particular angle possesses zero

intensity.¹⁴ A comparable phenomenon was found earlier in acoustics for diffraction on a corrugated surface.¹⁸

Analysis of the data in Fig. 5(a) proves that the interval of angles $23^\circ < \varphi \leq \varphi_C$ is characterized by abrupt changes of the reflection coefficients. This interval includes two characteristic points, one of which is the Brewster angle φ_{B2} , while the other one is the critical angle φ_C . As known, at $\varphi > \varphi_C$ there exists, in a crystal, only a single reflected acoustic wave characterized by the reflection coefficient equal to unity.¹ The performed calculations prove that, in tellurium dioxide, the magnitudes of the second Brewster and the critical angle are very close to each other $\varphi_{B2} \approx 24.130^\circ$ and $\varphi_C \approx 24.131^\circ$. Consequently, it is unlikely to distinguish between the two angles experimentally. As for the distribution of the elastic energy over the two reflected waves, it is reasonable to predict that, in the interval of the angles from $\varphi = 23^\circ$ to $\varphi_{B2} \approx 24.130^\circ$, the reflection coefficient R_2 rapidly approaches unity, while the energy flow of the extraordinary reflected beam vanishes. It means that the total reflection of the incident energy into the ordinary wave (2) may be expected in the specimen at $\varphi = \varphi_{B2}$. Finally, a further increase in the cut angle from φ_{B2} to the critical angle φ_C is accompanied by the abrupt drop of the energy of the ordinary wave ($R_2=0$). It results in inevitable jump of the energy in the backreflected wave (3), for which the coefficient R_3 changes from zero to $R_3=1$.

As for the critical angle φ_C , it can be predicted that all incident elastic energy is reflected from the boundary as the quasibackward wave (3). Moreover, the investigation confirms that the forward wave (2) disappears at $\varphi > \varphi_C$ because the supplementary dashed line in Fig. 3 intersects with the acoustic wave surface only at one point. It is also quite likely that the ordinary reflected wave at the critical angle $\varphi = \varphi_C$ becomes inhomogeneous (evanescent). The wave propagates with the energy flow directed along the border of the crystal. It is obvious that all cases of the reflection at the cut angle $\varphi > \varphi_C$ correspond to a single extraordinary reflected acoustic wave (3). The reflection coefficient R_3 in this case is equal to $R_3=1$. The energy flow of this wave practically meets the energy flow of the incident beam because the separation angle $\Delta\theta_3$ in Fig. 4 is limited to $\Delta\theta_3 \leq 10^\circ$ over a wide range of the cut angles.

Calculations prove that the behavior of the waves in mercury halides remains similar to that in tellurium dioxide. Corresponding dependences of the reflection coefficient in the compounds of mercury are plotted in Fig. 5(b). It is seen that absolute magnitudes of the critical angles are only slightly different from those in TeO_2 . For example, in calomel, the critical angle equals $\varphi_C=22.324^\circ$. On the other hand, it was found that, in calomel, the maximal value of the reflection coefficient of the backreflected wave is equal to $R_3=0.93$ and not to $R_3=1$, as in paratellurite. It means that it is not reasonable to predict the existence of the first Brewster angle in mercury crystals because their elastic anisotropy is not as strong as in TeO_2 . Nevertheless, the elastic anisotropy of the mercury materials is still sounding because the difference between the second Brewster angle φ_{B2} and the critical angle φ_C is negligibly small.

The carried out analysis proves that the unusual reflection of acoustic waves in the materials possessing moderate and low elastic anisotropy, for example, in TiO_2 and BaTiO_3 , may not be observed at all. This statement is confirmed by data presented in Figs. 5(c) and 5(d) and in Table II. As seen, the maximal magnitude of the reflection coefficient for the reflected wave (3) in TiO_2 and BaTiO_3 is very low, $R_3=0.43$ and $R_3=0.05$, respectively. The analysis also demonstrates that the magnitudes of the Brewster and the critical angles in the ferroelectric material appear smaller than in paratellurite and calomel: they are equal to $\varphi_{B2}=14.1^\circ$ and $\varphi_C=14.3^\circ$ in TiO_2 while $\varphi_{B2}=8.1^\circ$ and $\varphi_C=9.7^\circ$ in BaTiO_3 . Consequently, the difference between these two angles in TiO_2 and BaTiO_3 is quite noticeable in comparison with tellurium dioxide or calomel. Moreover, the reflected wave (3) in barium titanate propagates at the angle $\Delta\theta_3$ exceeding 70° , i.e., far away from the energy flow of the incident wave. That is why the quasi-back-reflection of elastic waves in the commonly used acoustic crystals does not exist.

A similar analysis was carried out for the case of the fast acoustic modes in the crystals. It was found that, in a wide range of the cut angles in paratellurite, a major amount of the incident elastic energy is transformed into a quasishear wave. The maximal value of the reflection coefficient for this wave approaches a unit $R_3=0.94$. The reflection in TeO_2 samples cut at the angles close to $\varphi=90^\circ$ is characterized by growth of the energy of the quasilongitudinal wave and by total decrease in the energy in the quasishear wave. In general, this reflection, contrary to the reflection of the quasishear waves, takes place in accordance with the expectations. It means that the Brewster and the critical angles may not be observed in the crystals. It also means that mutual distribution of elastic energy over the reflected waves changes continuously, i.e., without abrupt drops.

VIII. CONCLUSIONS

Basic results of the carried out analysis in tetragonal crystals are summarized in Table II. The examined crystal-line materials are listed in the table in accordance with the anisotropy of their elastic properties. The ratio of the maximal and minimal acoustic phase velocity values r was used to describe the anisotropy quantitatively. It is seen in the table that the walk-off angle between the phase and group velocities of ultrasound increases with the growth of the parameter A . As found, the propagation of bulk acoustic waves in the crystalline materials possessing strong anisotropy of elastic properties may be accompanied by a peculiar quasi-back-reflection of the acoustic energy flux from a free surface separating the crystals and the surrounding vacuum. The angle between the incident and backreflected energy flows in the crystals may be as narrow as a few degrees. In commonly used materials, the angle is wider.

The major peculiarity of the examined case of acoustic reflection consists of the fact that the unusual reflection follows the process of glancing incidence of elastic waves on a free and flat boundary separating a crystal and the vacuum. This type of reflection was, up until now, practically not investigated in acoustic crystals and other anisotropic media.

As proved by the investigation and seen in Table II, the relative intensity of the extraordinary reflected waves depends on the elastic anisotropy of the crystals. In acousto-optic crystals with strong anisotropy, e.g., in tellurium dioxide and mercury halides, the efficiency of the unusual reflection may be as high as 1.00, i.e., 100%. On the other hand, in traditional acoustic materials with moderate anisotropy, the effect of backreflection is relatively weak. In crystals with a low grade of anisotropy, the unusual reflection of elastic energy is absent. Therefore, it may be stated that the greater the anisotropy the stronger the effect of backacoustic reflection.

It may also be concluded that the unusual cases of acoustic reflection are interesting not only from the point of view of physical acoustics but also of other fundamental sciences, optics, magnetism, and the theory of waves. It is reasonable to expect the existence of similar reflection phenomena in anisotropic media of another physical nature, e.g., in polymers, magnetic films, ionosphere, etc.¹⁹ Observation of the examined effects may also be expected in nanomaterials. Finally, it is clear that new types of acoustoelectronic and acousto-optic instruments may be designed based on the examined effects.^{8–12,20} Tunable acousto-optic filters with collinear and noncollinear propagations of beams as well as acoustoelectronic delay lines with low consumption of expensive crystalline materials are the most evident examples of the possible applications.

ACKNOWLEDGMENTS

The work of N.V.P. is supported in part by the grant of the President of the Russian Federation for young scientists MK-1358.2008.8.

- ¹B. A. Auld, *Acoustic Fields and Waves in Solids* (Krieger, New York, 1990).
- ²E. Dieulesaint and D. Royer, *Ondes Elastiques dans les Solides (Elastic Waves in Solids)* (Masson, Paris, 1974).
- ³A. Goutzoulis and D. Pape, *Design and Fabrication of Acousto-Optic Devices* (Dekker, New York, 1994).
- ⁴J. C. Kastelik, M. G. Gazalet, C. Bruneel, and E. Bridoux, "Acoustic shear wave propagation in paratellurite with reduced spreading," *J. Appl. Phys.* **74**, 2813–2817 (1993).
- ⁵M. Gottlieb, A. Goutzoulis, and N. Singh, "High-performance acousto-

- optical materials: Hg₂Cl₂ and PbBr₂," *Opt. Eng. (Bellingham)* **31**, 2110–2117 (1992).
- ⁶M. J. P. Musgrave, "Refraction and reflection of plane elastic waves at a plane boundary between aeolotropic media," *Geophys. J. R. Astron. Soc.* **3**, 406–418 (1960).
- ⁷E. G. Lean and W. H. Chen, "Large angle beam steering in acoustically anisotropic crystal," *Appl. Phys. Lett.* **35**, 101–103 (1979).
- ⁸V. B. Voloshinov, "Close to collinear acousto-optical interaction in paratellurite," *Opt. Eng. (Bellingham)* **31**, 2089–2094 (1992).
- ⁹V. B. Voloshinov, "Anisotropic light diffraction on ultrasound in a tellurium dioxide single crystal," *Ultrasonics* **31**, 333–338 (1993).
- ¹⁰J. Sapriel, D. Charissoux, V. B. Voloshinov, and V. Molchanov, "Tunable acousto-optic filters and equalizers for WDM applications," *J. Lightwave Technol.* **20**, 888–896 (2002).
- ¹¹V. B. Voloshinov and N. V. Polikarpova, "Application of acousto-optic interactions in anisotropic media for control of light radiation," *Acust. Acta Acust.* **89**, 930–935 (2003).
- ¹²V. B. Voloshinov and N. V. Polikarpova, "Collinear tunable acousto-optic filters applying acoustically anisotropic material tellurium dioxide," *Molecular and Quantum Acoustics*, **24**, 225–235 (2003).
- ¹³N. V. Polikarpova and V. B. Voloshinov, "Intensity of reflected acoustic waves in acousto-optic crystal tellurium dioxide," *Proc. SPIE* **5828**, 25–36 (2004).
- ¹⁴V. B. Voloshinov, N. V. Polikarpova, and V. G. Mozhaev, "Nearly backward reflection of bulk acoustic waves at grazing incidence in a TeO₂ crystal," *Acoust. Phys.* **52**, 297–305 (2006); "Близкое к обратному отражение объемных акустических волн при скользящем падении в кристалле парателлурита", *Akust. Zh.* **52**, 245–251 (2006).
- ¹⁵V. B. Voloshinov, O. Yu. Makarov, and N. V. Polikarpova, "Nearly backward reflection of elastic waves in an acousto-optic crystal of paratellurite," *Tech. Phys. Lett.* **31**, 79–87 (2005); "Близкое к обратному отражение волн в акустооптическом кристалле парателлурита," *Pis'ma Zh. Tekh. Fiz.* **31**, 352–355 (2005).
- ¹⁶N. V. Polikarpova and V. B. Voloshinov, "Glancing incidence and back reflection of elastic waves in tetragonal crystals" *Proc. SPIE* **5953**, 0C1–0C12 (2005).
- ¹⁷A. V. Zakharov, N. V. Polikarpova, and E. Blomme, "Intermediate regime of light diffraction in media with strong elastic anisotropy" *Proc. SPIE* **5953**, 0D1–0D10 (2005).
- ¹⁸N. F. Declercq, R. Briers J. Degrieck, and O. Leroy "Diffraction of horizontally polarized ultrasonic plane waves on a periodically corrugated solid-liquid interface for normal incidence and Brewster angle incidence," *IEEE Trans. Ultrason. Ferroelectr. Freq. Control* **49**, 1516–1521 (2002).
- ¹⁹N. F. Declercq, J. Degrieck, and O. Leroy, "Sound in biased piezoelectric materials of general anisotropy," *Ann. Phys.* **14**, 705–722 (2005).
- ²⁰N. F. Declercq, N. V. Polikarpova, V. B. Voloshinov, O. Leroy, and J. Degrieck, "Enhanced anisotropy in paratellurite for inhomogeneous waves and its possible importance in the future development of acousto-optic devices," *Ultrasonics* **44**, 833–837 (2006).